1997 IEEE International Conference on Robotics and Automation, April 21-27, Albuquerque, NM.

Modeling and Identification of an Electrohydraulic Articulated Forestry Machine

Evangelos Papadopoulos[1], Bin Mu[1], and Real Frenette[1,2]

[1]Department of Mechanical Engineering & Centre for Intelligent Machines
McGill University, Montreal, PQ, Canada H3A 2A7
[2]Centre de Recherche Informatique de Montréal (CRIM), Montreal, PQ, Canada H3A 2N4

Abstract

This paper focuses on modeling and parameter estimation for the electrohydraulic actuation system of an articulated forestry machine. The linear graph method is implemented in deriving mathematical models of the swing, boom and stick subsystems. Actuation dynamics are subsequently integrated with manipulator dynamics to result in a complete machine model. Identification procedures employed in estimating physical parameters are discussed. Model validation studies show good agreement between model predictions and experiments. The derived models will be used for designing a controller for coordinated endpoint motion, for prediction, and for a real-time graphical training simulator.

1 Introduction

Forestry is Canada's most important industry in terms of people employed and contribution to the economy, [1]. However, increased competition from overseas and strict environmental laws require that forestry resources are harvested more efficiently and more carefully than previously. This requires sophisticated forestry equipment with better and easier-to-use controls, increased efficiency, and self-diagnostics. Such equipment will allow operators to concentrate more at planning tree harvesting operations.

However, sophistication or inclusion of computerized control and diagnostics should not increase costs significantly, and the system should remain reliable in harsh environments. These requirements dictate the use of industrial grade computers and hydraulic actuation systems; i.e. high-end workstations and expensive servovalves are not appropriate. Improving performance can be obtained in part by modeling and model-based control. An important challenge is how to use industrial grade technology to achieve results possible with high performance robotic systems. In particular, in this paper we are concerned with modeling the electrohydraulic actuation system of an experimental forestry machine, see Fig. 1, for the purposes of control, prediction, and use in a graphical training simulator [2].

Mathematical models are extensively used towards understanding the dynamic characteristics of electrohydraulic actuation systems for designing and implementing control algorithms. The majority of previous work has focused on modeling of individual servovalves, transmission lines and actuators. Mclain *et al* [3] developed dynamic models for a complete electrohydraulic actuation system. However, the models included a single-stage, four-way, suspension-type valve, not used in industry. The high cost of hydraulics including sensors and data-acquisition systems, and the lack of experience in hydraulics, have limited research on heavy-duty hydraulics. Because of these reasons, control design and coordination of articulated manipulators are not easy to achieve [4]. Nevertheless, various identification methods for transmission lines [5], [6], actuators [7], and servovalves [8], [9], have been proposed and implemented, and specific servo actuation systems have been investigated [3], [10].

In this paper, we study the dynamic behavior of the electrohydraulic system of a forestry machine. The linear graph method is implemented in deriving mathematical models of three actuation subsystems used on the vehicle, namely, the swing, boom and stick subsystems. Then the actuation dynamics are integrated with manipulator dynamics to result in a complete machine model. Identification procedures employed in estimating physical parameters are discussed. Model validation studies show good agreement between the model and experiments. Therefore, the derived models can be used as a valuable tool in the analysis and control of electrohydraulic actuation systems.

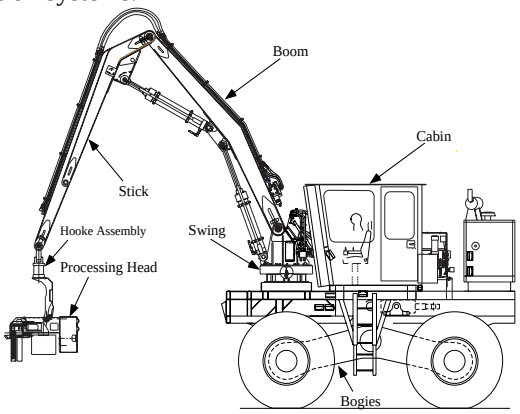

Fig. 1. The FERIC forestry machine.

2 The Experimental Forestry Machine

The work described here is part of a recent Canadian initiative in forestry robotics, called 'ATREF' (Application des Technologies Robotiques aux Équipements Forestiers) [2]. The machine used was provided by the Forest Engineering Research Institute of Canada (FERIC), and is equipped with an articulated manipulator which includes a

hydraulic motor-actuated swing joint, and cylinder-actuated boom and stick joints. An end-point Hooke-type assembly permits free swinging of the processing head in two degrees of freedom (dofs), see Fig. 1. The actuators operate at 3,000 psi, provided by two constant-pressure pumps which, in turn, are driven by a diesel engine, rated 152 hp at 2,500 rpm. Commands, issued by an on-board operator, are processed and sent to actuators by an embedded computer system.

3 System Modeling

The dynamic characteristics of the hydraulic systems are intricate due to the large number of components involved and their nonlinear behavior. To achieve the desired level of accuracy in modeling and estimating the corresponding parameters, the system was broken into its components. Each of these is modeled individually, and the overall dynamic model is assembled from the individual models. The components modeled here include pumps, proportional valves, hoses, cylinders and the swing motor. Linear graphs are chosen as the modeling methodology [15].

(a) Pumps. Two pressure-compensated, piston pumps provide constant pressure to the test vehicle, and are modeled as ideal pressure sources, see Figs. 2 and 3.

(b) Valves. Three two-stage, four-way proportional spool valves are used to actuate the swing, boom and stick subsystems. Only the resistive effect of the valves is considered in the dynamic models, due to the fact that their natural frequency is much higher than that of the hydraulics and manipulator. It is also assumed that the fluid and the geometry of the valve are ideal (e.g. sharp edges), [11]. The valve resistance, is given by the orifice equation

$$\Delta P = C_R \cdot Q \cdot |Q| \tag{1}$$

where the coefficient C_R is a function of fluid density ρ, the orifice area *A*, and the discharge coefficient C_d,

$$C_R = \frac{\rho}{2 \cdot C_d{}^2 \cdot A^2} \tag{2}$$

Input voltage commands modulate the orifice areas, which in turn, affect the magnitude of C_R. For most sliding-type valves at small openings, C_d is fairly constant when the Reynolds number is greater than 260. If the orifice edges are sharp, as assumed previously, $C_d = 0.60$ to 0.65, [12].

(c) Hoses. Lumped-parameter modeling methodology is applied to derive transmission line models. Their validity depends on whether the frequency of oscillation in the actuation system is significantly less than the frequency corresponding to wave propagation, [13]. Therefore, if *f* is the frequency of oscillation, and *l* is the line length, then a lumped parameter analysis is valid provided that

$$f < \frac{C_0}{2\pi l}, \text{ with } C_0 = \sqrt{\frac{\beta}{\rho}} \tag{3}$$

where C_o is the velocity of sound in the fluid, and β is its bulk modulus. For the fluid used $\beta = 1.6 \times 10^9 N/m^2$, $\rho = 970\ kg/m^3$, and for the longest hose on the test vehicle (4 meters), the wave propagation frequency *f* is 51 Hz, which is far above the frequencies possibly occurring in the actuation system. Therefore, only one lump is required for any of the hoses used on the experimental vehicle.

Several modeling assumptions were made: (a) Turbulent flow is assumed (non-linear pressure-flow relationship) for the boom and stick. In contrast, laminar flow is assumed for the swing model due to the fact that the swing hoses are very short, and turbulent flow can not develop completely, (b) Fluid compressibility and line compliance effects are linear. They hold for relatively small pressure fluctuations from the steady state pressure and for small expansions in the hoses, (c) In defining fluid inertance, the momentum of the fluid on the inlet and outlet sides of a control volume is assumed to be the same. There are many alternatives of arranging inertance, capacitance and resistance elements for a hose model. A common 'T' type is used, in which the resistance and inertance are in series, and the capacitance is connected at their common node, see Figs 2 and 3.

(d) Hydraulic cylinders. Two single-ended (asymmetrical) type of cylinders are used to actuate the boom and stick. It is assumed that cylinder chambers are rigid, that dominant friction effects in the piston seals are viscous, (the oil lubricates the seals and greatly reduces the effect of coulomb friction), and that there is no significant leakage past the piston; this is further prevented by the piston single-ended configuration. Since hydraulic cylinders convert fluid to mechanical power, this transduction is modeled as a gyrator. Due to the single-ended configuration, the common two-port element gyrator can not be applied directly. Instead, two two-port gyrators are used, see Fig. 3.

(e) Hydraulic motor. A fixed-displacement, piston motor is used to drive the swing. Contrary to cylinders, hydraulic motors can be modeled easily as single two-port gyrators, see Fig. 2. Several assumptions are made as follows. (1) Viscous friction of the motor is lumped into the damping of the gear train connected to its output shaft. (2) Internal and external motor leakage is present, and slip flow is laminar. Although, in general, the volumetric efficiency of hydraulic motors is quite high, at low speeds the slip flow effect becomes more prominent. Very often, the swing motor is working within this speed range.

(f) Other components. Filters and check valves are present which behave as fluid resistances. However, specifications show that their resistance is much smaller compared to that of the valves, actuators and hoses. Therefore, their effect is neglected.

Based on the above, the linear graph of the swing subsystem was constructed as shown in Fig. 2. In this figure, P_s is the pump pressure; C_R, $C_{R'}$ the valve orifice resistance modulated by the input voltage; I_1, I_2, C_1, C_2 and R_1, R_2, are the supply and return line inertance, capacitance and resistance, R_{in}, R_{e1}, R_{e2} the internal and external leakage of the motor whose volumetric displacement is D_m, N is the gear train gear ratio, B_{sw} is the gear train viscous damping, and $\dot{q}_{sw}$ the swing angular velocity.

Similarly, the boom and stick models are constructed as shown in Fig. 3. Additional parameters include, the rod

and head areas of the piston, $gy_1 = A_1$ and $gy_2 = A_2$., the viscous cylinder damping B, and $\dot{x}$ the piston velocity.

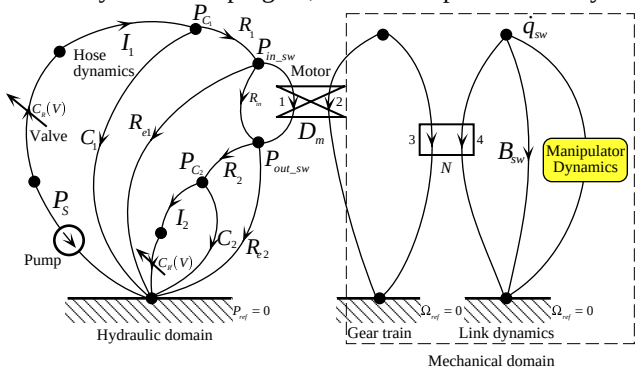

Fig. 2. The swing subsystem model.

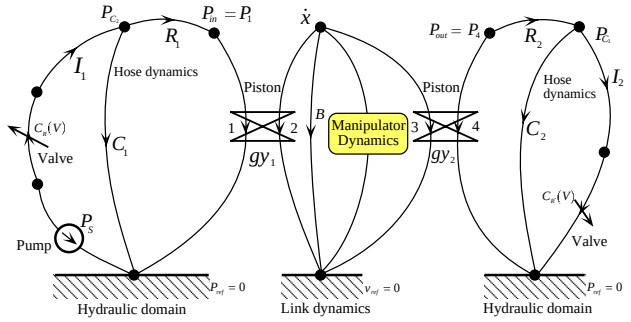

Fig. 3. Boom and stick linear graphs.

The dynamic models of the manipulator, were derived separately, and have the form [14]

$$\mathbf{M(q)}\cdot\ddot{\mathbf{q}} + \mathbf{V(q,\dot{q})} + \mathbf{G(q)} = \boldsymbol{\tau} \tag{4}$$

where **M(q)** is a mass matrix, **V(q,$\dot{\mathbf{q}}$)** includes Coriolis and centrifugal terms, **G(q)** includes gravity terms, and $\boldsymbol{\tau}$ is the input torque provided by the actuators. To integrate this model to the hydraulic actuator models, one needs to provide expressions transforming pressure differences to forces or torques, and angular velocities to flows.

For the two cylinders, one can write

$$\dot{\mathbf{x}} = \mathbf{J}\cdot\dot{\mathbf{q}}, \quad \boldsymbol{\tau}_{cyl} = \mathbf{J}^{\mathbf{T}}\cdot\mathbf{F} \tag{5}$$

where **x** is the vector of piston displacements, **q** is the vector of manipulator joint angles, **F** includes the forces generated by the actuators, and $\boldsymbol{\tau}_{cyl}$ are the corresponding torques. Since each link is independently actuated, the Jacobian **J** is a diagonal matrix.

For single-ended type of cylinders, we have

$$\begin{bmatrix} F_{bm} \\ F_{sk} \end{bmatrix} = \begin{bmatrix} A_{in\_bm} & -A_{out\_bm} & 0 & 0 \\ 0 & 0 & A_{in\_sk} & -A_{out\_sk} \end{bmatrix} \begin{bmatrix} P_{in\_bm} \\ P_{out\_bm} \\ P_{in\_sk} \\ P_{out\_sk} \end{bmatrix} \tag{6a}$$

$$\begin{bmatrix} Q_{in\_bm} \\ Q_{in\_sk} \\ Q_{out\_bm} \\ Q_{out\_sk} \end{bmatrix} = -\begin{bmatrix} A_{in\_bm} & 0 \\ 0 & A_{in\_sk} \\ A_{out\_bm} & 0 \\ 0 & A_{out\_sk} \end{bmatrix} \begin{bmatrix} \dot{x}_{bm} \\ \dot{x}_{sk} \end{bmatrix} \tag{6b}$$

where A_{in_bm}, A_{out_bm}, A_{in_sk}, A_{out_sk} are driving and returning areas of the boom and stick pistons; F_{bm}, F_{sk} are the forces generated by boom and stick cylinders. Similarly, P_{in_bm}, P_{out_bm}, P_{in_sk}, P_{out_sk} are pressures at inlet and outlet of the boom and stick cylinders, and Q_{in_bm}, Q_{out_bm}, Q_{in_sk}, Q_{out_sk} are flow rates. The negative sign in the second equation is due to linear graph conventions. Therefore, the transduction equations can be written as

$$\begin{bmatrix} \tau_{bm} \\ \tau_{sk} \end{bmatrix} = \boldsymbol{\tau}_{cyl} = \mathbf{J}^T(\mathbf{q})\cdot\mathbf{F} = \mathbf{J}^T(\mathbf{q})\cdot\begin{bmatrix} F_{bm} \\ F_{sk} \end{bmatrix}$$

$$= \mathbf{J}^T\begin{bmatrix} A_{in\_bm} & -A_{out\_bm} & 0 & 0 \\ 0 & 0 & A_{in\_sk} & -A_{out\_sk} \end{bmatrix}\begin{bmatrix} P_{in\_bm} \\ P_{out\_bm} \\ P_{in\_sk} \\ P_{out\_sk} \end{bmatrix} \tag{7a}$$

$$\begin{pmatrix} \dot{q}_{bm} \\ \dot{q}_{sk} \end{pmatrix} = \mathbf{J}^{-1}\begin{bmatrix} \dot{x}_{bm} \\ \dot{x}_{sk} \end{bmatrix} = -\mathbf{J}^{-1}\begin{bmatrix} 1/A_{in\_bm} & 0 \\ 0 & 1/A_{in\_sk} \end{bmatrix}\begin{bmatrix} Q_{in\_bm} \\ Q_{in\_sk} \end{bmatrix}$$

$$= -\mathbf{J}^{-1}\begin{bmatrix} 1/A_{out\_bm} & 0 \\ 0 & 1/A_{out\_sk} \end{bmatrix}\begin{bmatrix} Q_{out\_bm} \\ Q_{out\_sk} \end{bmatrix} \tag{7b}$$

The transduction equation for the swing motor is more standard, and including the gear train results in

$$\begin{bmatrix} \dot{q}_{sw} \\ \tau_{sw} \end{bmatrix} = \begin{bmatrix} 0 & 1/(D_m N) \\ -D_m N & 0 \end{bmatrix}\begin{bmatrix} P_{in\_sw} - P_{out\_sw} \\ Q_{sw} \end{bmatrix} \tag{8}$$

The relationship between manipulator dynamics, in terms of variables $\boldsymbol{\tau}$ and $\dot{\mathbf{q}}$ and electrohydraulic actuator dynamics, in terms of variables **P , Q** are set up. The overall dynamic equations for the three dof manipulator are given below.

$$\dot{\mathbf{q}}_1 = \mathbf{q}_2$$

$$\dot{\mathbf{q}}_2 = \mathbf{M}(\mathbf{q}_1)^{-1}\left\{-\mathbf{V}(\mathbf{q}_1,\mathbf{q}_2) - \mathbf{G}(\mathbf{q}_1) + \tau\right\}$$

$$\dot{P}_{c_1\_sw} = \left(Q_{i_1\_sw} - \left(P_{C_1\_sw} - P_{R_{in}}(\dot{q}_{sw}) - P_{R_2} - P_{C_2\_sw}\right)/R_1\right)/C_{1\_sw}$$

$$\dot{P}_{c_2\_sw} = \{\left(P_{C_1\_sw} - P_{R_{in}}(\dot{q}_{sw}) - P_{R_2} - P_{C_2\_sw}\right)/R_1 -$$
$$\left(P_{R_{in}}(\dot{q}_{sw}) + P_{R_2} + P_{C_2\_sw}\right)/R_{e1}$$
$$-\left(P_{C_2\_sw} + P_{R_2}\right)/R_{e2} - Q_{i_2\_sw}\}/C_{2\_sw}$$

$$\dot{Q}_{i_1\_sw} = \left(P_s - C_R\cdot Q_{i_1\_sw}{}^2\cdot sign(Q_{i_1\_sw}) - P_{C_1\_sw}\right)/I_{1\_sw}$$

$$\dot{Q}_{i_2\_sw} = \left(P_{C_2\_sw} - C_{R'}\cdot Q_{i_2\_sw}{}^2\cdot sign(Q_{i_2\_sw})\right)/I_{2\_sw}$$

$$\dot{P}_{c_1\_bm} = \left(Q_{i_1\_bm} - gy_1\cdot\dot{x}_{bm}\right)/C_{1\_bm}$$

$$\dot{P}_{c_2\_bm} = \left(gy_2\cdot\dot{x}_{bm} - Q_{i_2\_bm}\right)/C_{2\_bm} \tag{9a}$$

$$\dot{Q}_{i_1\_bm} = \left(P_s - C_R\cdot Q_{i_1\_bm}{}^2\cdot sign\left(Q_{i_1\_bm}\right) - P_{c_1\_bm}\right)/I_{1\_bm}$$

$$\dot{Q}_{i_2\_bm} = \left(P_{c_2\_bm} - C_{R'}\cdot Q_{i_2\_bm}{}^2\cdot sign\left(Q_{i_2\_bm}\right)\right)/I_{2\_bm}$$

$$\dot{P}_{c_1\_sk} = \left(Q_{i_1\_sk} - gy_1\cdot\dot{x}_{sk}\right)/C_{1\_sk}$$

$$\dot{P}_{c_2\_sk} = \left(gy_2\cdot\dot{x}_{sk} - Q_{i_2\_sk}\right)/C_{2\_sk}$$

$$\dot{Q}_{i_1\_sk} = \left(P_s - C_R\cdot Q_{i_1\_sk}{}^2\cdot sign\left(Q_{i_1\_sk}\right) - P_{c_1\_sk}\right)/I_{1\_sk}$$

$$\dot{Q}_{i_2\_sk} = \left(P_{c_2\_sk} - C_{R'}\cdot Q_{i_2\_sk}{}^2\cdot sign\left(Q_{i_2\_sk}\right)\right)/I_{2\_sk}$$

where

$$\mathbf{q_1} = \begin{bmatrix} q_{sw} & q_{bm} & q_{sk} \end{bmatrix}^T, \quad \boldsymbol{\tau} = \begin{bmatrix} \tau_{sw} & \tau_{bm} & \tau_{sk} \end{bmatrix}^T \qquad (9b)$$

4 Experimental Identification

The majority of the parameters were identified individually in order to minimize estimation errors. The damping associated with the joints was estimated using least squares techniques after all other parameters were identified. Various types of sensors were used for the experiments, as depicted in Fig. 4. The data-acquisition system is based on a STD32-bus Ziatech-8902, 486 DX-2 computer installed at the back of the cabin on the vehicle, see Fig. 4. This embedded system, is running QNX real-time operating system. The data sampling rate can reach as high as 200 Hz. The data was collected and sent to a remote 486 DX-2 computer, also running QNX.

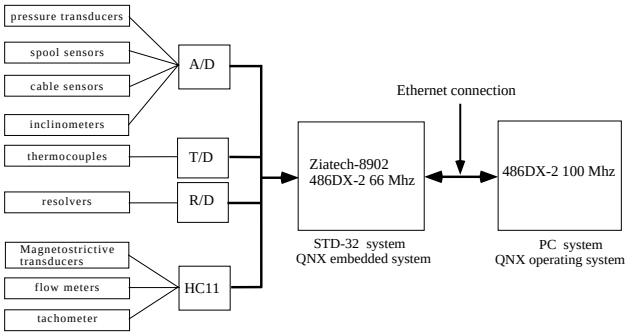

Fig. 4. The data acquisition system structure.

(a) *Valves*. The objective is to estimate the relationship between voltage input V and the C_R factor. Since the three valves used for the swing, boom and stick are identical, only one of them is tested and its C_R measured. By varying the magnitude of input voltage commands, several sets of pressures P_{in}, P_{out} and flow rates Q were collected. Using Eq. (1) and a MATLAB curve fitting algorithm, a polynomial representation of $C_R(V)$ was found, see Fig. 5.

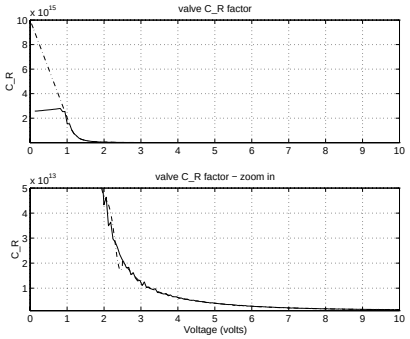

Fig. 5. Valve characteristics.

In this figure, solid lines indicate experimental results and dotted lines results from curve fitting. The flat region between 0 and 1 volts is due to flow sensor limitations.

(b) *Hose resistance*. For incompressible, fully developed turbulent flow in hoses, pressure drop is related to flow according to Eq. (1). By varying valve orifice, flow rates and corresponding pressure differences across a SAE 100R12 hose of 4 meters in length and 3/4" in diameter were measured, and the results are plotted in Fig. 6. In this figure, the solid line represents experimental measurements and the dotted line is the polynomial curve fitting result (C_R = 3.125e^{-11} Pa/(m^3/sec)^2). The flat region at the beginning of the solid line is due to flow meter limitations.

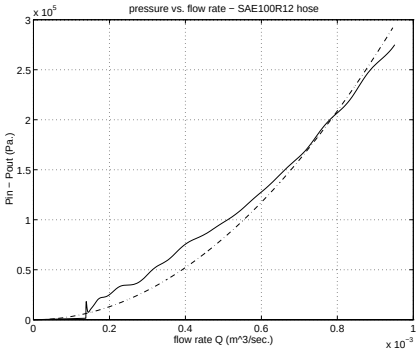

Fig. 6. Hose resistance measurement.

The SAE 100R12 very-high-pressure hydraulic hose is the only type of hose used on the vehicle. For hoses with different diameters and lengths, their resistance can be calculated using the following exact formula, [12]

$$\Delta P = \alpha \frac{\mu^{0.25} \rho^{0.75} L}{D^{4.75}} Q^{1.75} \Rightarrow \frac{\Delta P}{Q^{1.75}} \propto \frac{L}{D^{4.75}} \qquad (10)$$

where α is a constant depending on the units, μ is the absolute viscosity, ρ is the fluid density, L is the pipe length, and D is the inside diameter of the pipe. To obtain a new C_R, $Q^{1.75}$ is approximated by $Q \cdot |Q|$, [15].

(c) Inertance and capacitance. The fluid inertance and capacitance are estimated from the pressure and flow rate readings according to their definitions.

For a machine hose with length of 4 meters and diameter of 3/4", four groups of data were collected. The mean values of the inertance and capacitance are calculated from each group of data. The final result was obtained as the average of these four mean values, see Fig. 7.

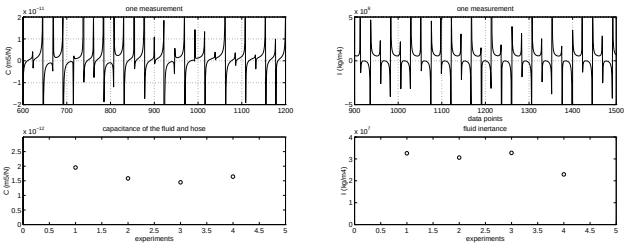

$C = 1.585 \times 10^{-12} m^5 / N$ $\quad I = 3.062 \times 10^7 kg / m^4$

Fig. 7. Hose capacitance & inertance estimation.

(d) *Motor leakage*. Two types of leakage flows exist in motors: the internal or cross-port leakage between higher and lower pressure chambers, and the external leakage from each motor chamber passing through the pistons to the case drain. Because all clearances in a motor are intentionally made small to reduce losses, these leakage flows are laminar and, therefore, proportional to the pressure differences.

The internal leakage is proportional to the pressure difference across the inlet and outlet ports of a motor, and can be written as

$$\Delta P = P_1 - P_2 = R_{in} \cdot Q_{in} \tag{11}$$

where R_{in} is the internal or cross-port leakage resistance, and ΔP is the pressure difference across the motor ports.

The external leakage in each piston chamber is proportional to the chamber pressure and can be written as:

$$P_1 = R_{ex} \cdot Q_{ex1}, \quad P_2 = R_{ex} \cdot Q_{ex2} \tag{12}$$

where R_{ex} is the external resistance, P_1 is the pressure in forward chamber and P_2 is pressure in return chamber. The experimental results are displayed in Fig. 8.

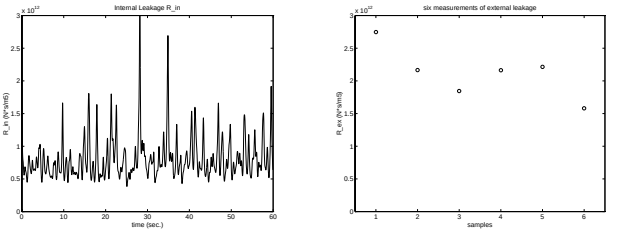

$R_{in} = 8.002 \times 10^{11}\, N \cdot s / m^5$ $\quad$ $R_{ex} = 2.119 \times 10^{12}\, N \cdot s / m^5$

Fig. 8. Internal and external motor leakage.

(d) *Damping coefficients in cylinders and motor*. The physical connections of the manipulator prevent the actuators from being disconnected from the arm and base. Since we can not estimate the viscous damping B without considering the effect of other physical parameters, viscous friction is estimated after other parameters are identified, and the accumulative errors are lumped into them.

By assuming all the other parameters are known, $\ddot{\mathbf{q}} = \mathbf{M(q)}^{-1} \cdot \left(-\mathbf{V(q,\dot{q})} - \mathbf{G(q)} + \boldsymbol{\tau}\right)$ can be reformulated into the form of $\dot{q}_{sw} \cdot B = a$ for the swing subsystem, and $\dot{x} \cdot B = a$ for the boom and stick subsystems. Using a least squares approach and many experimental sets results in

$$\mathbf{B} = \left[\dot{\mathbf{q}}^{\mathrm{T}}\dot{\mathbf{q}}\right]^{-1}\dot{\mathbf{q}}^{\mathrm{T}}\mathbf{a} \;\text{ or }\; \mathbf{B} = \left[\dot{\mathbf{x}}^{\mathrm{T}}\dot{\mathbf{x}}\right]^{-1}\dot{\mathbf{x}}^{\mathrm{T}}\mathbf{a} \tag{13}$$

The values of the damping coefficients are given in Fig. 9.

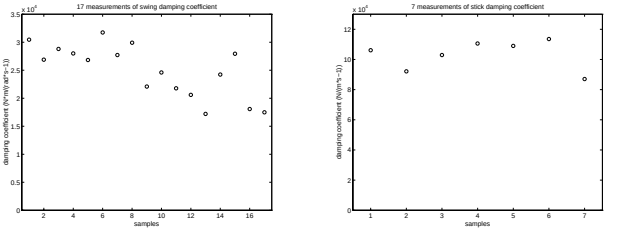

$B_{sw} = 2.450 \times 10^{4}\, N \cdot m / (rad \cdot s^{-1})$ $\quad$ $B_{sk} = 1.030 \times 10^{5}\, N / (m \cdot s^{-1})$

Fig. 9. Damping estimation for the gear train and the stick cylinder.

5 Model Validation

(a) The swing subsystem. The input commands to the swing subsystem and its actual and predicted values of the system variables are shown in Fig. 10. The solid line stands for actual measurements and the dotted line is the prediction using the derived dynamic models by simulation.

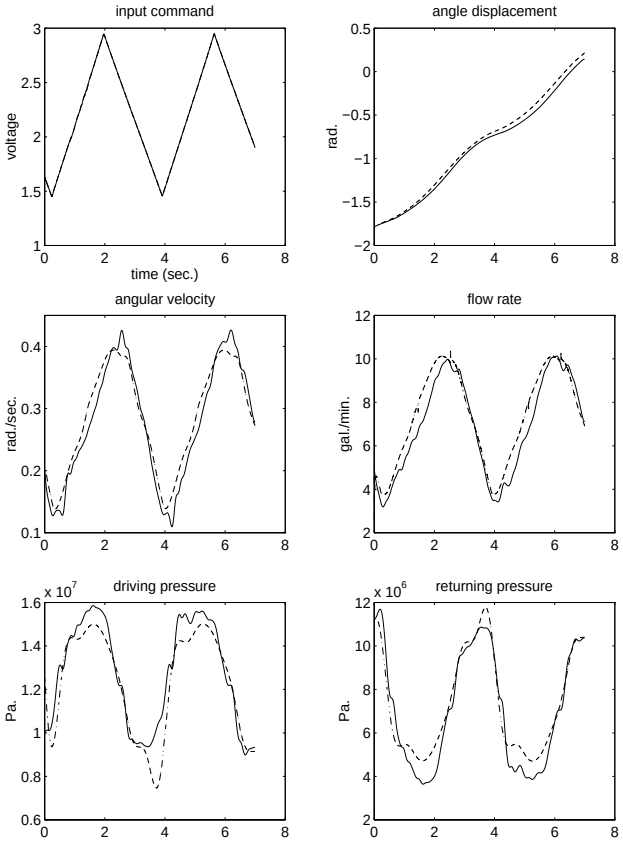

Fig. 10. Swing model validation studies.

The prediction of angular displacements and velocities is very close to the actual ones. The flow rate prediction is also very good because of its relationship to angular velocity. The predicted pressure profiles are close to the real ones, although part of the peaks were underestimated. The inertia properties were estimated using AutoCad [14]. Any discrepancies between the actual and the calculated mass properties could cause inaccuracies in the estimation of the inertia matrix. Furthermore, just before the experiments were conducted, a 2-DOF Hooke-type pendulum attachment was added to the stick endpoint. Periodic motions of the manipulator caused swinging motions of this attachment. Although its mass properties were known, the dynamic effects of this motion were neglected due to the lack of sensors. A more accurate friction model might also contribute in improving the results.

(b) The stick subsystem. The actual input to the stick subsystem and the actual and predicted values of some system variables are shown in Fig. 11. Overall, predicted responses are good, especially for the angle displacement and derivatives. Again, minor discrepancies can be attributed to the same reasons as above. The 2-DOF pendulum mechanism was assumed to be a point mass in the dynamic models used. Its inertia properties, which have a bigger effect on the stick than on the swing, are not taken into account here. In addition, the overall inertia properties of the stick need to be reconsidered. The reason for the

bumpy shape of the returning pressure is still not clear. They could be attributed to the fact that the system includes single-ended cylinders with non-equal areas and valves with symmetrical spools.

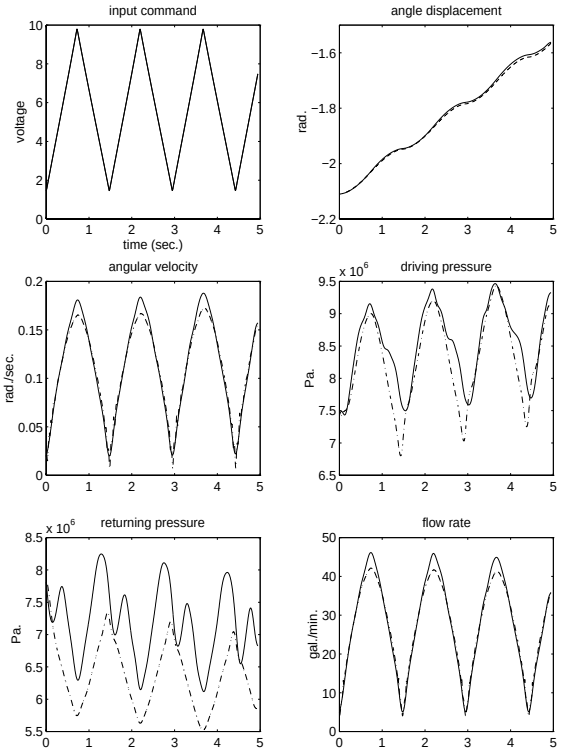

Fig. 11. Model validation for the stick.

Although some do discrepancies exist in the prediction of the stick return pressure, the main objective of this study was to provide good predictions for angle displacements and joint angular velocities. Consequently, both the swing, boom and stick models are well-behaved and sufficient. The model will be tested further during control design.

6 Conclusions

In this paper, we developed models for the electrohydraulic system of a forestry machine. The linear graph method was implemented in deriving mathematical models for the swing, boom and stick subsystems. The actuation dynamics were integrated with manipulator dynamics to result in a complete machine model. Estimation procedures employed in obtaining values of physical parameters were discussed. Model validation studies showed good agreement between the model and experiments. The derived models will be used for control, prediction, and training simulator purposes.

Acknowledgments

The financial support for this work by the Ministère de l'Industrie, du Commerce, de la Science et de la Techno-logie of Quebec, (MICST), under the program SYNERGIE is gratefully acknowledged. Also, the authors wish to thank P. Freedman (CRIM), I. Makkonen (FERIC), R. Germain and J. LeBrun (Denharco), and D. Éthier, and R. Lessard (Autolog) for their help in various aspects of this work.

References

[1] Courteau, J., "Robotics in Canadian Forestry," *IEEE Canadian Review*, Winter 1994, pp. 10-13.

[2] Freedman, P., Papadopoulos, E., Poussart, D., Gosselin, C., and Courteau, J, "ATREF: Application des Technologies Robotiques aux Équipements Forestiers," *Proc. 1995 Canadian Conf. on Electrical and Computer Engineering*, Montreal, PQ, Sept. 5-8, 1995.

[3] McLain, T. W., et al., "Development, Simulation, and Validation of a Highly Nonlinear Hydraulic Servosystem Model," *American Control Conf.* Pittsburgh, Pennsylvania, June 1989, pp. 385-391.

[4] Zhou, J. J., Conrad, F., "Identification for Modeling and Adaptive Control of Hydraulic Robot Manipulators," *Identification & System Parameter Estimation 1991*, No. 2, 1992, pp. 705-710.

[5] Yang, W. C., Tobler, W. E., "Dissipative Modal Approximation of Fluid Transmission lines Using Linear Friction Model," *Dynamic Systems, Measurement, & Control*, Vol. 113, 1991, pp. 152-161.

[6] Krus, P., Weddfelt, K., Palmberg, J., "Fast Pipeline Models for Simulation of Hydraulic Systems," *Journal of Dynamic Systems, Measurement, and Control*, Vol. 116, 1994, pp. 132-136.

[7] Wells, D. L., et al., "An Investigation of Hydraulic Actuator Performance Trade-Offs Using a Generic Model," *Proc. IEEE Int. Conf. on Robotics and Automation*, 1990, pp. 2168-2173.

[8] Martin, D. J., Burrow, C. R., "The Dynamic Characteristics of an Electrohydraulic Servovalve," *Journal of Dynamic Systems, Measurement, and Control*, 1976.

[9] Nikiforuk, P. N., et al., "Detailed Analysis of a Two-Stage Four-Way Electrohydraulic Flow-Control Valve," *Journal of Mechanical Engineering Science*, Vol. 11, No. 2, 1969.

[10] Herman, T., et al., "Bond-Graph Modeling and Identification of a High Power Hydraulic System," *11th IASTED Int. Conf. Modeling, Identification and Control*, Innsbrunk, Austria, 1992.

[11] Blackburn, J. F., et al., *Fluid Power Control*. Technology Press of M.I.T. and John Willey, 1960.

[12] Merritt, H. E., *Hydraulic Control Systems*. John Willey & Sons, 1967.

[13] Watton, J., *Fluid Power Systems*, Pr. Hall, 1989.

[14] Sarkar, S., "*Dynamic Modeling of an Articulated Forestry Machine for Simulation and Control*," Master's Thesis, Dept. of Mech. Eng., McGill University, Montreal, 1996.

[15] Mu, B., "*System Modeling, Identification and Coordinated Control Design for an Articulated Forestry Machine*," Master's Thesis, Dept. of Mech. Eng., McGill University, Montreal, 1996.